Adaptive Spacecraft Formation Flying with Actuator Saturation

Anton. H. J. de Ruiter *

Carleton University

4925 Colonel By Drive, Ottawa, ON K1S 5B6, Canada

aderuite@mae.carleton.ca

Abstract

This paper presents a nonlinear adaptive controller for the multiple spacecraft formation flying problem. The formulation allows for gravitational field models of arbitrary order, and a broad class of linearly parameterized external disturbance force models. This paper builds upon previous results using feedback of the filtered error. Making use of Barbalat's lemma, a broad class of controllers feeding back the filtered error is obtained, which encompasses the linear feedback that is typically used in the literature. In particular, conditions are presented under which the linear feedback is asymptotically stable under actuator saturation. The resulting controller performance is demonstrated with a numerical simulation for a relative orbit under J2 perturbations.

Keywords

spacecraft formation flying, adaptive control, actuator saturation constraints

*Anton de Ruiter is an Assistant Professor at Carleton University

1 Introduction

The coordinated flight of multiple spacecraft in formation is topic of significant current interest [1, 2, 3]. Multiple spacecraft formation flying has been identified by NASA and the U.S. Air Force as an enabling technology for future missions. The ability to accurately control the relative positions of the spacecraft is key to the success of such missions. Several different control design approaches have been applied to the formation control problem, such as the Linear Quadratic Regulator [4], intelligent control [5], decentralized control [6], coordinated and synchronized control [7, 8, 9] and adaptive control [10, 11, 12]. For these methods to be practically useful, they must work under realistic conditions including (but not limited to) sensor errors, measurement rate, and communication delays. In particular, given the limited thrust available, a significant realistic limitation is actuator saturation. Gurfil et al. [12] addresses this issue in the context of deep space spacecraft formation flying using a Model Reference Adaptive Controller with pseudocontrol hedging. This paper focusses on the aspect of actuator saturation for the application of the Slotine and Li adaptive controller ([13]) to spacecraft formation flying, which first appeared in [10].

The Slotine and Li adaptive controller has been applied to tracking problems in various applications such as spacecraft attitude control, control of robotic systems, control of spacecraft formations, and makes use of the filtered error [10, 13, 14, 15, 16]. The filtered error may be defined as follows. Given the state vector $\boldsymbol{p}(t) \in R^n$, the filtered error is defined as

$$\boldsymbol{r}(t) \stackrel{\Delta}{=} \dot{\boldsymbol{p}}(t) + \boldsymbol{\Lambda}\boldsymbol{p}(t), \tag{1}$$

where $\boldsymbol{\Lambda} > \boldsymbol{0}$ is some positive-definite matrix.

There are various results in the literature relating conditions on the filtered error

$\boldsymbol{r}(t)$ to asymptotic convergence of the state vector $\boldsymbol{p}(t) \rightarrow \mathbf{0}$. The ones that seem to be used the most rely on the condition that $\boldsymbol{r}(t) \in \mathcal{L}_2$ (see for example [16, 17]). The need to show that $\boldsymbol{r}(t) \in \mathcal{L}_2$ typically leads to linear feedback of the filtered error, ($\boldsymbol{u} = -\mathbf{K}\boldsymbol{r}$ with $\mathbf{K} > \mathbf{0}$) (see for example [16, 10]). This means that the available control actuation must be unlimited. In practise, this is not the case, and the available control actuation is limited. It would be desirable to obtain control laws that are stable in the presence of actuator saturation. As mentioned in [13, 14, 15], convergence of the filtered error $\boldsymbol{r}(t) \rightarrow \mathbf{0}$ by itself guarantees convergence of the state vector $\boldsymbol{p}(t) \rightarrow \mathbf{0}$. However, in these papers, only linear feedback of the filtered error is considered. In this paper, this fact will be used to obtain a much larger class of stabilizing controllers for the adaptive spacecraft formation flying problem, of which the linear feedback are a subset. In particular, asymptotic stability in the presence of actuator saturation will be shown.

In [10], the formulation is for two spacecraft flying in a two-body gravitational field. As mentioned in [10], it is straightforward to extend this formulation to arbitrary gravitational fields. Because no significant extra effort is needed to do this, it will be done so here. Additionally, in [10], the disturbance forces on each spacecraft are assumed to be constant. This may not be entirely realistic. Again, because it requires no significant extra effort, this will be generalized here to allow any form of disturbance forces, provided they can be parameterized linearly with constant coefficients (for example, fourier series).

2 Preliminary Mathematical Results

In this paper, wherever the norm of a vector appears, it will be taken to be the 2-norm, that is $\|\boldsymbol{x}\| = \sqrt{\boldsymbol{x}^T\boldsymbol{x}}$. Wherever the norm of a matrix appears, it will be taken to be the induced 2-norm, that is $\|\mathbf{X}\| = \sqrt{\lambda_{max}(\mathbf{X}^T\mathbf{X})}$, where

$\lambda_{max}(\cdot)$ denotes the maximum eigenvalue.

The main result on the filtered error from [13] is now stated.

Lemma 1:

Consider the filtered error in (1). Then, $\boldsymbol{r}(t) \rightarrow \mathbf{0}$ as $t \rightarrow \infty$ if and only if $\dot{\boldsymbol{p}}(t) \rightarrow \mathbf{0}$ and $\boldsymbol{p}(t) \rightarrow \mathbf{0}$ as $t \rightarrow \infty$.

Another useful result that will be needed is contained in the following proposition.

Proposition 1

Let the function $\boldsymbol{f}(\boldsymbol{x}, t) : R^n \times R \rightarrow R^m$ be uniformly continuous in $\boldsymbol{x}$, uniformly in t, and uniformly continuous in t, uniformly in $\boldsymbol{x}$. Then, given any uniformly continuous function $\boldsymbol{y}(t) : R \rightarrow R^n$, the function $\boldsymbol{g}(t) \stackrel{\Delta}{=} \boldsymbol{f}(\boldsymbol{y}(t), t)$ is uniformly continuous in t.

Proof

Let $\boldsymbol{y}(t)$ be any uniformly continuous function in t. Then, given any $\epsilon > 0$, $\exists \delta_{fx} > 0$, $\exists \delta_{ft} > 0$ such that $\|\boldsymbol{x}_2 - \boldsymbol{x}_1\| < \delta_{fx} \Rightarrow \|\boldsymbol{f}(\boldsymbol{x}_2, t) - \boldsymbol{f}(\boldsymbol{x}_1, t)\| < \frac{\epsilon}{2}$, $\forall t \in R$ and $|t_2 - t_1| < \delta_{ft} \Rightarrow \|\boldsymbol{f}(\boldsymbol{x}, t_2) - \boldsymbol{f}(\boldsymbol{x}, t_1)\| < \frac{\epsilon}{2}$, $\forall \boldsymbol{x} \in R^n$. By uniform continuity of $\boldsymbol{y}(t)$, $\exists \delta_{yt} > 0$ such that $|t_2 - t_1| < \delta_{yt} \Rightarrow \|\boldsymbol{y}(t_2) - \boldsymbol{y}(t_1)\| < \delta_{fx}$. Now, $\|\boldsymbol{f}(\boldsymbol{y}(t_2), t_2) - \boldsymbol{f}(\boldsymbol{y}(t_1), t_1)\| \leq \|\boldsymbol{f}(\boldsymbol{y}(t_2), t_2) - \boldsymbol{f}(\boldsymbol{y}(t_2), t_1)\| + \|\boldsymbol{f}(\boldsymbol{y}(t_2), t_1) - \boldsymbol{f}(\boldsymbol{y}(t_1), t_1)\|$. By choosing $\delta = \min(\delta_{yt}, \delta_{ft})$, and making use of the above results, $|t_2 - t_1| < \delta \Rightarrow \|\boldsymbol{g}(t_2) - \boldsymbol{g}(t_1)\| < \epsilon$. This completes the proof. □

3 Spacecraft Formation Flying Dynamics

In this section, the spacecraft formation flying problem is formulated. The formulation is similar to that in [10].

As in [10], a leader/follower type of formation will be considered. The leader may or may not be an actual spacecraft. It could simply be a reference point on the orbit that the follower is controlled relative to. As shown in Figure 1, the same reference frame as in [10] will be used, with the y-axis pointing away from the center of the earth, the z-axis pointing in the orbit angular momentum direction, and the x-axis pointing nominally in the negative velocity direction, completing the right-handed triad.

The relative dynamics can be expressed in the orbiting frame as [10]

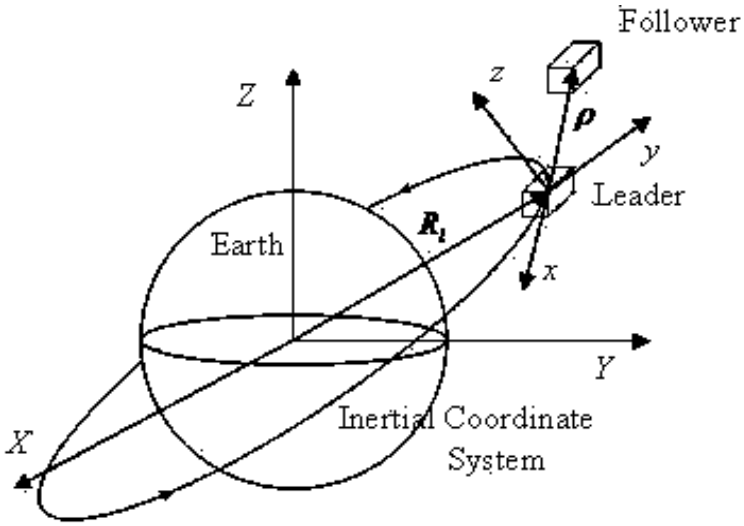

Figure 1: Orbiting Reference Frame

$$\begin{aligned} m_f\ddot{\boldsymbol{\rho}} &= -m_f\left(2\boldsymbol{\omega}_o^{\times}\dot{\boldsymbol{\rho}} + \boldsymbol{\omega}_o^{\times}\boldsymbol{\omega}_o^{\times}\boldsymbol{\rho} + \dot{\boldsymbol{\omega}}_o^{\times}\boldsymbol{\rho}\right) \\ &\quad + m_f\left(\boldsymbol{a}_g(\boldsymbol{R}_f) - \boldsymbol{a}_g(\boldsymbol{R}_l)\right) + \boldsymbol{u}_f - \tfrac{m_f}{m_l}\boldsymbol{u}_l + \boldsymbol{f}_{fd} - \tfrac{m_f}{m_l}\boldsymbol{f}_{ld}, \end{aligned} \tag{2}$$

where m_f and m_l are the follower and leader mass, $\boldsymbol{R}_f$ and $\boldsymbol{R}_l$ are the follower and leader inertial position, $\boldsymbol{\omega}_o$ is the angular velocity of the orbiting frame, $\boldsymbol{a}_g(\boldsymbol{R})$ is the gravitational acceleration, $\boldsymbol{u}_f$ and $\boldsymbol{u}_l$ are the follower and leader control forces, $\boldsymbol{f}_{fd}$ and $\boldsymbol{f}_{ld}$ are the disturbance forces on the follower and leader,

and $\boldsymbol{\rho} = \boldsymbol{R}_f - \boldsymbol{R}_l$ is the relative position.

Assumption 1

It is assumed that the differential disturbance force can be parameterized linearly as

$$\boldsymbol{f}_{fd} - \frac{m_f}{m_l}\boldsymbol{f}_{ld} = -\mathbf{W}(\boldsymbol{\rho}, t)\boldsymbol{\theta}, \tag{3}$$

for some constant vector $\boldsymbol{\theta} \in R^d$, and some mapping $\mathbf{W}(\boldsymbol{\rho}, t) : R^3 \times R \to R^{3\times d}$, such that for any $d > 0$, $\boldsymbol{\rho} \in \mathcal{B}_d$ implies $\exists \bar{w} > 0$ such that $\|\mathbf{W}(\boldsymbol{\rho}, t)\| \leq \bar{w}, \forall t \geq 0$, where $\{\mathcal{B}_d \triangleq \boldsymbol{x} \in R^3 : \|\boldsymbol{x}\| \leq d\}$. Additionally, $\mathbf{W}(\boldsymbol{\rho}, t)$ is assumed to be continuous in $\boldsymbol{\rho}$ uniformly in t and uniformly continuous in t uniformly in $\boldsymbol{\rho}$.

Since the spacecraft masses are typically known very accurately, they are not estimated (unlike in [10]).

4 Formulation of Control Law

As in [10], it is assumed that a desired relative spacecraft trajectory $\boldsymbol{\rho}_d(t)$ is available, and that $\boldsymbol{\rho}_d(t)$ and its first two derivatives are continuous and bounded. The relative position error is defined as

$$\boldsymbol{e}(t) \triangleq \boldsymbol{\rho}(t) - \boldsymbol{\rho}_d(t). \tag{4}$$

The control objective is then to ensure that $\boldsymbol{e}(t) \to \mathbf{0}$ as $t \to \infty$. In order to make use of the results in section 2, the filtered error is defined as

$$\boldsymbol{r}(t) \triangleq \dot{\boldsymbol{e}}(t) + \boldsymbol{\Lambda}\boldsymbol{e}(t), \tag{5}$$

for some constant positive definite diagonal design parameter $\mathbf{\Lambda} > \mathbf{0}$. Differentiating (5) leads to

$$\begin{aligned} \dot{\boldsymbol{r}}(t) &\triangleq \ddot{\boldsymbol{e}}(t) + \mathbf{\Lambda}\dot{\boldsymbol{e}}(t), \\ &= \ddot{\boldsymbol{\rho}} - \ddot{\boldsymbol{\rho}}_d + \mathbf{\Lambda}\dot{\boldsymbol{e}}(t). \end{aligned} \tag{6}$$

Multiplying (6) by m_f and substituting (2) gives

$$\begin{aligned} m_f\dot{\boldsymbol{r}} &= -m_f\left(\ddot{\boldsymbol{\rho}}_d(t) - \mathbf{\Lambda}\dot{\boldsymbol{e}}(t)\right) - m_f\left(2\boldsymbol{\omega}_o^{\times}\dot{\boldsymbol{\rho}} + \boldsymbol{\omega}_o^{\times}\boldsymbol{\omega}_o^{\times}\boldsymbol{\rho} + \dot{\boldsymbol{\omega}}_o^{\times}\boldsymbol{\rho}\right) \\ &\quad -m_f\left(\boldsymbol{a}_g(\boldsymbol{R}_l) - \boldsymbol{a}_g(\boldsymbol{R}_f)\right) - \tfrac{m_f}{m_l}\boldsymbol{u}_l - \left(-\boldsymbol{f}_{fd} + \tfrac{m_f}{m_l}\boldsymbol{f}_{ld}\right) + \boldsymbol{u}_f. \end{aligned}$$

From this it is readily seen that

$$m_f\dot{\boldsymbol{r}} = -\bar{\boldsymbol{u}}_{ff} - \mathbf{W}(\boldsymbol{\rho}, t)\boldsymbol{\theta} + \boldsymbol{u}_f, \tag{7}$$

where

$$\begin{aligned} \bar{\boldsymbol{u}}_{ff} &= m_f\left(\ddot{\boldsymbol{\rho}}_d(t) - \mathbf{\Lambda}\dot{\boldsymbol{e}}(t)\right) + m_f\left(2\boldsymbol{\omega}_o^{\times}\dot{\boldsymbol{\rho}} + \boldsymbol{\omega}_o^{\times}\boldsymbol{\omega}_o^{\times}\boldsymbol{\rho} + \dot{\boldsymbol{\omega}}_o^{\times}\boldsymbol{\rho}\right) \\ &\quad +m_f\left(\boldsymbol{a}_g(\boldsymbol{R}_l) - \boldsymbol{a}_g(\boldsymbol{R}_f)\right) + \tfrac{m_f}{m_l}\boldsymbol{u}_l. \end{aligned}$$

Since the parameters contained in $\boldsymbol{\theta}$ are unknown, the control law is chosen to have the form

$$\boldsymbol{u}_f = \bar{\boldsymbol{u}}_{ff} + \mathbf{W}(\boldsymbol{\rho}, t)\hat{\boldsymbol{\theta}}(t) + \bar{\boldsymbol{u}}_f, \tag{8}$$

where $\bar{\boldsymbol{u}}_f$ is a to be determined feedback term, and $\hat{\boldsymbol{\theta}}(t)$ is an estimate of $\boldsymbol{\theta}$, which is obtained from the adaptation law

$$\dot{\hat{\boldsymbol{\theta}}} = -\mathbf{\Gamma}\mathbf{W}^T\boldsymbol{r}, \tag{9}$$

where $\mathbf{\Gamma} > \mathbf{0}$ is some constant positive definite matrix. Defining the adaptation error to be $\tilde{\boldsymbol{\theta}} \triangleq \boldsymbol{\theta} - \hat{\boldsymbol{\theta}}$, the adaptation error dynamics become

$$\dot{\tilde{\boldsymbol{\theta}}} = \mathbf{\Gamma} \mathbf{W}^T \boldsymbol{r}, \tag{10}$$

and substituting the control (8) into (7) gives the filtered error dynamics

$$m_f \dot{\boldsymbol{r}} = -\mathbf{W}(\boldsymbol{\rho}, t)\tilde{\boldsymbol{\theta}} + \bar{\boldsymbol{u}}_f. \tag{11}$$

Now, all that remains is to choose the feedback part of the control, $\bar{\boldsymbol{u}}_f$.

Assumption 2

The class of feedback control laws considered in this paper is.

$$\bar{\boldsymbol{u}}_f = \boldsymbol{g}(\boldsymbol{r}, t), \tag{12}$$

where $\boldsymbol{g}(\boldsymbol{r}, t)$ is continuous in $\boldsymbol{r}$ uniformly in t, uniformly continuous in t uniformly in $\boldsymbol{r}$, and for any $d > 0$, $\boldsymbol{r} \in \mathcal{B}_d$ implies $\exists \bar{g} > 0$ such that $\|\boldsymbol{g}(\boldsymbol{r}, t)\| \leq \bar{g}, \forall t > 0$, where $\{\mathcal{B}_d \triangleq \boldsymbol{x} \in R^3 : \|\boldsymbol{x}\| \leq d\}$.

The result in Lemma 2 leads to a large class of asymptotically stabilizing control laws as demonstrated in the following theorem.

Theorem 1

Let Assumption 1 be satisfied. Consider the control and adaptation laws in (8) and (9) respectively. Assume that the leader control $\boldsymbol{u}_l$ is bounded, and that the leader spacecraft orbital position $\boldsymbol{R}_l$ evolves on the set $\mathcal{R}_o \triangleq \{\boldsymbol{R} \in R^3 : R_{min} \leq \|\boldsymbol{R}\|$ for some $R_{p,max} < R_{min}$, where $R_{p,max}$ is the maximum radius of the planet including atmosphere (if it has one). Assume that the desired relative position $\boldsymbol{\rho}_d$ is chosen such that the desired follower orbital position $(\boldsymbol{R}_l + \boldsymbol{\rho}_d) \in \mathcal{R}_o$

also. Assume that the initial conditions satisfy $\|\boldsymbol{e}(0)\| + \frac{\bar{r}}{\underline{\lambda}} \leq R_{min} - R_{p,max}$, where $\bar{r} = \sqrt{\frac{2V(\boldsymbol{r}(0),\tilde{\boldsymbol{\theta}}(0))}{m_f}}$, $V(\boldsymbol{r},\tilde{\boldsymbol{\theta}}) \triangleq \frac{1}{2}m_f\boldsymbol{r}^T\boldsymbol{r} + \frac{1}{2}\tilde{\boldsymbol{\theta}}^T\boldsymbol{\Gamma}^{-1}\tilde{\boldsymbol{\theta}}$ and $\underline{\lambda} > 0$ is the minimum diagonal entry in $\boldsymbol{\Lambda}$. Let the feedback control law satisfy Assumption 2, such that $\forall \boldsymbol{r} \neq \boldsymbol{0}$, $\exists \epsilon(||\boldsymbol{r}||) > 0$ such that $\inf_{t\in[0,\infty)} -\boldsymbol{r}^T\boldsymbol{g}(\boldsymbol{r},t) \geq \epsilon$. Then, the closed-loop system is stable, with

$$\dot{\boldsymbol{e}}(t) \to \boldsymbol{0}, \;\; \boldsymbol{e}(t) \to \boldsymbol{0}$$

as $t \to \infty$.

Proof

Consider the Lyapunov-like function defined by

$$V(\boldsymbol{r},\tilde{\boldsymbol{\theta}}) \triangleq \frac{1}{2}m_f\boldsymbol{r}^T\boldsymbol{r} + \frac{1}{2}\tilde{\boldsymbol{\theta}}^T\boldsymbol{\Gamma}^{-1}\tilde{\boldsymbol{\theta}}.$$

Differentiating this along the trajectories of (11) and (10) leads to

$$\dot{V} = \boldsymbol{r}^T\boldsymbol{g}(\boldsymbol{r},t) \leq 0. \tag{13}$$

From this, it can be concluded that

$$V(t) \leq V(0), \;\; \forall t \geq 0, \tag{14}$$

and that both $\boldsymbol{r}(t)$ and $\tilde{\boldsymbol{\theta}}(t)$ are bounded, and hence the system is stable. Since $\boldsymbol{r}(t)$ is bounded, so are $\dot{\boldsymbol{e}}(t)$ and $\boldsymbol{e}(t)$ [17]. Since $\boldsymbol{\rho}_d, \dot{\boldsymbol{\rho}}_d$ are bounded, so are $\boldsymbol{\rho}, \dot{\boldsymbol{\rho}}$. Since $\boldsymbol{\rho}$ is bounded, Assumption 1 gives that $\mathbf{W}_d$ is also bounded. From (14) it can be concluded that $\|\boldsymbol{r}(t)\| \leq \;\bar{r}$. Now, from the definition of the filtered error,

$$\boldsymbol{e}(t) = e^{-\boldsymbol{\Lambda}t}\boldsymbol{e}(0) + e^{-\boldsymbol{\Lambda}t}\int_0^t e^{\boldsymbol{\Lambda}\tau}\boldsymbol{r}(\tau)d\tau.$$

This leads to the inequality $\|\boldsymbol{e}(t)\| \leq \|\boldsymbol{e}(0)\| + \frac{\bar{r}}{\underline{\lambda}}$. Now, the orbital position of the follower spacecraft is given by $\mathbf{R}_f = \mathbf{R}_l + \boldsymbol{\rho}_d + \boldsymbol{e}$. From this, it can be concluded that

$$R_{p,max} \leq R_{min} - \left(\|\boldsymbol{e}(0)\| + \frac{\bar{r}}{\underline{\lambda}} \right) \leq \|\mathbf{R}_f\|.$$

This shows that neither of the spacecraft collide with the planet, or enter its atmosphere.

By Assumption 2, $\boldsymbol{g}(\boldsymbol{r}, t)$ is also bounded. Therefore, from (11) it can be concluded that $\dot{\boldsymbol{r}}$ is bounded. Hence, $\boldsymbol{r}$ is a bounded uniformly continuous function of time. Since $\boldsymbol{r}$ is bounded, $\boldsymbol{r}(t) \in D, \ \forall t$ for some compact set D. Therefore, $\boldsymbol{g}(\boldsymbol{r}, t)$ is uniformly continuous in $\boldsymbol{r}$, uniformly in t on the set $\boldsymbol{r} \in D$, and uniformly continuous in t, uniformly in $\boldsymbol{r}$. By Proposition 1, $\boldsymbol{g}(\boldsymbol{r}(t), t)$ is itself uniformly continuous and bounded in time. Therefore, the product $\boldsymbol{r}^T(t)\boldsymbol{g}(\boldsymbol{r}(t), t)$ is uniformly continuous in time. From (14) and (13) the integral $\int_0^\infty \boldsymbol{r}^T(t)\boldsymbol{g}(\boldsymbol{r}(t), t)\, dt$ exists and is finite. Therefore, by Barbalat's Lemma [20], it can be concluded that $\boldsymbol{r}^T(t)\boldsymbol{g}(\boldsymbol{r}(t), t) \to 0$ as $t \to \infty$. Since $\forall \boldsymbol{r} \neq \mathbf{0}$, $\exists \epsilon(||\boldsymbol{r}||) > 0$ such that $\inf_{t\in[0,\infty)} -\boldsymbol{r}^T\boldsymbol{g}(\boldsymbol{r}, t) \geq \epsilon$, it must be that $\boldsymbol{r} \to \mathbf{0}$ as $t \to \infty$. Finally, Lemma 1 yields the result $\dot{\boldsymbol{e}} \to \mathbf{0}, \ \boldsymbol{e} \to \mathbf{0}$ as $t \to \infty$. This concludes the proof.

□

Remark 1: It can be seen that the class of stabilizing feedback controllers in Theorem 1 contains the class of controllers $\boldsymbol{u} = -\mathbf{K}\boldsymbol{r}$ with $\mathbf{K} > \mathbf{0}$, which are typically obtained using an $\boldsymbol{r}(t) \in \mathcal{L}_2$ argument.

Remark 2: The initial condition requirements, and the requirement related to the set $\mathcal{R}_o$ in Theorem 1 are technical conditions required for the result to hold. However, they are easily satisfied for any realistic planet orbiting formation.

Having obtained the result in Theorem 1, the case when actuator limitations

are present can now be treated.

Assumption 3

It is assumed that the available control is limited by

$$-\boldsymbol{u}_{max} \leq \boldsymbol{u}_f \leq \boldsymbol{u}_{max}, \tag{15}$$

where the inequality in (15) is taken componentwise, and $\boldsymbol{u}_{max} > \mathbf{0}$.

Consider now the feedback control law

$$\bar{\boldsymbol{u}}_f = -\mathbf{K}\boldsymbol{r}, \tag{16}$$

where $\mathbf{K} = diag\{k_1, k_2, k_3\}$ with $k_i > 0,\ i = 1, 2, 3$. Under the saturation constraints in Assumption 3, the control law in (8) is now implemented as

$$\boldsymbol{u}_f = sat\left(\bar{\boldsymbol{u}}_{ff} + \mathbf{W}\hat{\boldsymbol{\theta}}(t) - \mathbf{K}\boldsymbol{r}, -\boldsymbol{u}_{max}, \boldsymbol{u}_{max}\right), \tag{17}$$

where the saturation function is defined componentwise as

$$sat\left(\boldsymbol{x}_i, \boldsymbol{x}_{min,i}, \boldsymbol{x}_{max,i}\right) \triangleq \begin{cases} \boldsymbol{x}_{max,i}, & \text{if } \boldsymbol{x}_i > \boldsymbol{x}_{max,i} \\ \boldsymbol{x}_i & \text{if } \boldsymbol{x}_{min,i} \leq \boldsymbol{x}_i \leq \boldsymbol{x}_{max,i} \\ \boldsymbol{x}_{min,i} & \text{if } \boldsymbol{x}_i < \boldsymbol{x}_{min,i} \end{cases} \tag{18}$$

Before proceeding, an additional assumption is needed.

Assumption 4

The desired relative spacecraft trajectory $\boldsymbol{\rho}_d$ is designed such that $-\boldsymbol{u}_{max} + \boldsymbol{\delta} \leq \bar{\boldsymbol{u}}_{ff} + \mathbf{W}\hat{\boldsymbol{\theta}}(t) \leq \boldsymbol{u}_{max} - \boldsymbol{\delta}$, where $\boldsymbol{\delta} = \delta \begin{bmatrix} 1 & 1 & 1 \end{bmatrix}^T$ for some $\delta > 0$.

Under Assumption 4, the control law in (17) becomes

$$\boldsymbol{u}_f = \bar{\boldsymbol{u}}_{ff} + \mathbf{W}\hat{\boldsymbol{\theta}}(t) + sat\left(-\mathbf{K}\boldsymbol{r}, \bar{\boldsymbol{u}}_{min}(t), \bar{\boldsymbol{u}}_{max}(t)\right), \tag{19}$$

where $\bar{\boldsymbol{u}}_{min}(t) \triangleq -\boldsymbol{u}_{max} - (\bar{\boldsymbol{u}}_{ff} + \mathbf{W}\hat{\boldsymbol{\theta}}(t))$ and $\bar{\boldsymbol{u}}_{max}(t) \triangleq \boldsymbol{u}_{max} - (\bar{\boldsymbol{u}}_{ff} + \mathbf{W}\hat{\boldsymbol{\theta}}(t))$ with $-2\boldsymbol{u}_{max} < \bar{\boldsymbol{u}}_{min}(t) \leq -\boldsymbol{\delta}$ and $2\boldsymbol{u}_{max} > \bar{\boldsymbol{u}}_{max}(t) \geq \boldsymbol{\delta}$. The result for spacecraft formation control including actuator saturation limitations can now be stated.

Theorem 2

Let Assumptions 1, 3 and 4 be satisfied. Consider the control and adaptation laws in (17) and (9) respectively. Assume that the leader control $\boldsymbol{u}_l$ is bounded and uniformly continuous, and that the leader spacecraft orbital position $\mathbf{R}_l$ is uniformly continuous and evolves on the set $\mathcal{R}_o \triangleq \{\mathbf{R} \in R^3 : R_{min} \leq \|\mathbf{R}\|\}$ for some $R_{p,max} < R_{min}$. Assume that the desired relative position $\boldsymbol{\rho}_d$ is chosen such that the desired follower orbital position $(\mathbf{R}_l + \boldsymbol{\rho}_d) \in \mathcal{R}_o$ also. Assume that the initial conditions satisfy $\|\boldsymbol{e}(0)\| + \frac{\bar{r}}{\underline{\lambda}} \leq R_{min} - R_{p,max}$, where $\bar{r} = \sqrt{\frac{2V(\boldsymbol{r}(0), \tilde{\boldsymbol{\theta}}(0))}{m_f}}$ and $\underline{\lambda} > 0$ is the minimum diagonal entry in $\boldsymbol{\Lambda}$. Then, the closed-loop system is stable, with

$$\dot{\boldsymbol{e}}(t) \to \mathbf{0}, \;\; \boldsymbol{e}(t) \to \mathbf{0}$$

as $t \to \infty$.

Proof

Setting $\boldsymbol{g}(\boldsymbol{r}, t) = sat\left(-\mathbf{K}\boldsymbol{r}, \bar{\boldsymbol{u}}_{min}(t), \bar{\boldsymbol{u}}_{max}(t)\right)$, it is clear that $\boldsymbol{g}(\boldsymbol{r}, t)$ is bounded. Letting $\underline{k}$ and $\bar{k}$ be the minimum and maximum diagonal entries in $\mathbf{K}$ respectively, and choosing $\epsilon(||\boldsymbol{r}||) = \underline{k}||\boldsymbol{r}||^2$ when $||\boldsymbol{r}|| \leq \frac{\delta}{\bar{k}}$, and $\epsilon(||\boldsymbol{r}||) = \underline{k}\delta^2$ when $||\boldsymbol{r}|| > \frac{\delta}{\bar{k}}$, it can readily be shown that $\inf_{t\in[0,\infty)} -\boldsymbol{r}^T\boldsymbol{g}(\boldsymbol{r}, t) \geq \epsilon$. Since all assumptions in Theorem 1 are satisfied, other than Assumption 2, all that is

needed to prove this theorem is to show that Assumption 2 holds also.

Following the proof of Theorem 1, it can be shown that $\boldsymbol{r}$, $\dot{\boldsymbol{r}}$, $\tilde{\boldsymbol{\theta}}$, $\boldsymbol{e}$, $\dot{\boldsymbol{e}}$, $\boldsymbol{\rho}$, $\dot{\boldsymbol{\rho}}$, $\mathbf{W}$ are all bounded. From (6), it can be obtained that $\ddot{\boldsymbol{e}}$ and $\ddot{\boldsymbol{\rho}}$ are bounded also. Hence, $\boldsymbol{r}$, $\boldsymbol{e}$, $\dot{\boldsymbol{e}}$, $\boldsymbol{\rho}$ and $\dot{\boldsymbol{\rho}}$ are all uniformly continuous. Since $\boldsymbol{\rho}$ is bounded and uniformly continuous, Assumption 1a together with Proposition 1 gives that $\mathbf{W}$ is uniformly continuous also.

Since $\boldsymbol{\theta}$ is constant, and $\tilde{\boldsymbol{\theta}}$ is bounded (from the proof of Theorem 1), $\hat{\boldsymbol{\theta}}$ is bounded also. From equation (9), $\dot{\hat{\boldsymbol{\theta}}}$ is bounded. Hence, $\hat{\boldsymbol{\theta}}$ is uniformly continuous also. Finally, the product $\mathbf{W}\hat{\boldsymbol{\theta}}$ is uniformly continuous since it is the product of bounded uniformly continuous functions. It can therefore be concluded that the saturation limits in (19), $\bar{\boldsymbol{u}}_{min}(t)$ and $\bar{\boldsymbol{u}}_{min}(t)$ are uniformly continuous.

The continuity requirements on $\boldsymbol{g}(\boldsymbol{r},t)$ will now be established componentwise. Each component of $\boldsymbol{g}(\boldsymbol{r},t)$ has the form $h(x,t) = sat\,(-kx, a(t), b(t))$ where $a(t) < 0$ and $b(t) > 0$ are uniformly continuous. Fixing t, it can be seen that $h(x,t)$ satisfies

$$|h(x_2,t) - h(x_1,t)| \leq k|x_2 - x_2|$$

Therefore, with t fixed, $h(x,t)$ is Lipshitz continuous and hence uniformly continuous, independently of t. Now, fix x, and choose any $\epsilon > 0$. By uniform continuity of $a(t)$ and $b(t)$, $\exists \delta_a > 0,\ \ \delta_b > 0$ such that

$$|t_2 - t_1| < \delta_a \Rightarrow |a(t_2) - a(t_1)| < \epsilon,$$

$$|t_2 - t_1| < \delta_b \Rightarrow |b(t_2) - b(t_1)| < \epsilon,$$

Define $\delta \stackrel{\Delta}{=} \min(\delta_a, \delta_b)$. Then,

$$|t_2 - t_1| < \delta \Rightarrow |a(t_2) - a(t_1)| < \epsilon,\ |b(t_2) - b(t_1)| < \epsilon.$$

There are now several cases to consider. Consider $x < 0$.

Case 1 $b(t_1) < -kx$ and $b(t_2) < -kx$.

In this case, $|h(x,t_2) - h(x,t_1)| = |b(t_2) - b(t_1)| < \epsilon$.

Case 2 $b(t_1) < -kx \leq b(t_2)$.

In this case, $|h(x,t_2) - h(x,t_1)| = |-kx - b(t_1)| \leq |b(t_2) - b(t_1)| < \epsilon$.

Case 3 $b(t_2) < -kx \leq b(t_1)$.

Swapping t_1 and t_2, this is the same as for case 2.

Case 4 $b(t_1) \geq -kx$ and $b(t_2) \geq -kx$.

In this case, $|h(x,t_2) - h(x,t_1)| = 0$.

The same conclusions can be reached for $x > 0$ by simply swapping the sign of inequality and replacing $b(t)$ with $a(t)$ in Cases 1 to 4 above. The case $x = 0$ is trivial, since $h(0,t) = 0$. Therefore, it can be concluded that given any $\epsilon > 0$, $\exists \delta > 0$ independently of x, such that

$$|t_2 - t_1| < \delta \Rightarrow |h(x,t_2) - h(x,t_1)| < \epsilon.$$

Therefore, Assumption 2 is satisfied, and from Theorem 1, the result is proved. □

Now, the question arises as to how to ensure that the condition in Assumption 4 is satisfied. Consider the ball $\mathcal{B}_{\underline{u}} = \{\boldsymbol{u} \in R^3 : \|\boldsymbol{u}\| < \underline{u} - \delta, \underline{u} = \min_{i=1,2,3}\{|\boldsymbol{u}_{max,i}|\}$. This is the largest open ball such that $\mathcal{B}_{\underline{u}} \subset \{\boldsymbol{u} \in R^3 : -\boldsymbol{u}_{max} + \boldsymbol{\delta} < \boldsymbol{u} < \boldsymbol{u}_{max} - \boldsymbol{\delta}\}$. Therefore, if it can be shown that $\bar{\boldsymbol{u}}_{ff} + \mathbf{W}\hat{\boldsymbol{\theta}} \in \mathcal{B}_{\underline{u}}$, then Assumption 4 is satisfied.

Lemma 2

Given bounds on the unknown parameters, the orbital angular velocity and its derivative

$$\|\boldsymbol{\theta}\| \leq \bar{\theta}, \tag{20}$$

$$\|\boldsymbol{\omega}_o\| \leq \bar{\omega}_o, \tag{21}$$

and

$$\|\dot{\boldsymbol{\omega}}_o\| \leq \bar{\dot{\omega}}_o, \tag{22}$$

given a function $\bar{w}(s) \geq 0$ such that

$$\|\mathbf{W}(\boldsymbol{\rho}, t)\| \leq \bar{w}(\|\boldsymbol{\rho}\|). \tag{23}$$

Let $\boldsymbol{\Gamma} = diag\{\gamma_i\},\ \gamma_i > 0,\ \ i = 1, ..., d$ be diagonal, and define

$$\bar{V} = \frac{1}{2} m_f \boldsymbol{r}^T(0)\boldsymbol{r}(0) + \frac{1}{2\underline{\gamma}} \bar{\tilde{\theta}}_0^2, \tag{24}$$

where $\underline{\gamma}$ is the smallest diagonal element of $\boldsymbol{\Gamma}_d$.

Assume that the feedback control $\boldsymbol{g}(\boldsymbol{r}, t)$ satisfies $\boldsymbol{r}^T \boldsymbol{g}(\boldsymbol{r}, t) \leq 0$ on the interval $t \in [0, t^*]$, for some $t^* > 0$. As shown in the proof of Theorem 1, during the interval $t \in [0, t^*]$ the leader and follower spacecraft evolve on the set

$$\bar{\mathcal{R}_o} \triangleq \left\{ \mathbf{R} \in R^3 : R_{min} - \left(\|\boldsymbol{e}(0)\| + \frac{1}{\underline{\lambda}} \sqrt{\frac{2\bar{V}}{m_f}} \right) \leq \|\mathbf{R}\| \right\}.$$

It is assumed that the gravitational acceleration $\boldsymbol{a}_g(\mathbf{R})$ is differentiable on this domain, and that a known bound $A_g > 0$ exists such that

$$\left\| \frac{\partial \boldsymbol{a}_g}{\partial \mathbf{R}^T}(\mathbf{R}) \right\| \leq A_g, \forall \mathbf{R} \in \bar{\mathcal{R}}_o. \tag{25}$$

Under the above conditions, if the desired relative trajectory $\boldsymbol{\rho}_d(t)$ is designed such that

$$\bar{W}_\theta \leq \underline{u} - \delta, \tag{26}$$

for some arbitrarily small $\delta > 0$, where $\underline{u} = min_{i=1,2,3}\{\boldsymbol{u}_{max,i}|\}$,

$$\begin{aligned}\bar{W}_\theta \quad \triangleq \quad & \left\|\ddot{\boldsymbol{\rho}}_d + 2\boldsymbol{\omega}_o^\times \dot{\boldsymbol{\rho}}_d + (\boldsymbol{\omega}_o^\times \boldsymbol{\omega}_o^\times + \dot{\boldsymbol{\omega}}_o^\times)\boldsymbol{\rho}_d + \boldsymbol{a}_g(\mathbf{R}_l) - \boldsymbol{a}_g(\mathbf{R}_l + \boldsymbol{\rho}_d)\right\| m_f \\ & + \tfrac{m_f}{\underline{\lambda}} \sqrt{\tfrac{2\bar{V}}{m_f}} \left[(\underline{\lambda} + \bar{\lambda})(2\bar{\omega}_o + \bar{\lambda}) + \bar{\omega}_o^2 + \bar{\dot{\omega}}_o + A_g\right] \\ & + m_f \|\boldsymbol{e}(0)\| \left[(2\bar{\omega}_o + \bar{\lambda})\bar{\lambda} + \bar{\omega}_o^2 + \bar{\dot{\omega}}_o + A_g\right] \\ & + \bar{w}(\bar{\rho}_d + \|\boldsymbol{e}(0)\| + \tfrac{1}{\underline{\lambda}}\sqrt{\tfrac{2\bar{V}}{m_f}}) \left[\bar{\theta}_d + \sqrt{2\bar{\gamma}\bar{V}}\right],\end{aligned} \tag{27}$$

and $\|\boldsymbol{\rho}_d(t)\| \leq \bar{\rho}_d$ is a known bound, then

$$\|\bar{\boldsymbol{u}}_{ff} + \mathbf{W}\hat{\boldsymbol{\theta}}\| \leq \bar{W}_\theta \leq \underline{u} - \delta. \tag{28}$$

on the interval $t \in [0, t^*]$. Note that $\bar{\lambda}$ and $\underline{\lambda}$ are the maximum and minimum diagonal entries of $\boldsymbol{\Lambda}$ respectively.

Proof The Lyapunov-like function in Theorem 1 is given by

$$V(t) = \frac{1}{2} m_f \boldsymbol{r}^T(t)\boldsymbol{r}(t) + \frac{1}{2}\tilde{\boldsymbol{\theta}}^T(t)\boldsymbol{\Gamma}^{-1}\tilde{\boldsymbol{\theta}}(t) \tag{29}$$

Given bounds on the initial estimation error, the Lyapunov-like function (29) can be upperbounded at its initial condition by $V(0) \leq \bar{V}$. Making use of (14) in the proof of Theorem 1, it can be shown that

$$\|\boldsymbol{r}(t)\| \leq \sqrt{\frac{2\bar{V}}{m_f}}, \tag{30}$$

$$\|\tilde{\boldsymbol{\theta}}(t)\| \leq \sqrt{2\bar{\gamma}\bar{V}}, \tag{31}$$

where $\bar{\gamma}$ is the largest diagonal element of $\mathbf{\Gamma}$. Following the proof of Theorem 1, (30) and the definition of the filtered error (1) leads to

$$\|\boldsymbol{e}(t)\| \leq \|\boldsymbol{e}(0)\| + \frac{1}{\underline{\lambda}}\sqrt{\frac{2\bar{V}}{m_f}}, \tag{32}$$

$$\|\dot{\boldsymbol{e}}(t)\| \leq \left(\frac{\underline{\lambda}+\bar{\lambda}}{\underline{\lambda}}\right)\sqrt{\frac{2\bar{V}}{m_f}} + \bar{\lambda}\|\boldsymbol{e}(0)\|. \tag{33}$$

Finally, the bounds (20) and (31), together with the definition of the adaptation error, lead to bounds on the estimates

$$\|\hat{\boldsymbol{\theta}}(t)\| \leq \bar{\theta} + \sqrt{2\bar{\gamma}\bar{V}}. \tag{34}$$

From (25), it can be obtained that

$$\|\boldsymbol{a}_g\left(\mathbf{R}_l(t) + \boldsymbol{\rho}_d(t)\right) - \boldsymbol{a}_g\left(\mathbf{R}_l(t) + \boldsymbol{\rho}_d(t) + \boldsymbol{e}(t)\right)\| \leq A_g\|\boldsymbol{e}(t)\|. \tag{35}$$

Since the leader satellite control $\boldsymbol{u}_l$ is essentially a free parameter, it can always be chosen so as to reduce $\|\bar{\boldsymbol{u}}_{ff} + \mathbf{W}\hat{\boldsymbol{\theta}}\|$. Therefore, in the following analysis, its contribution is ignored (set $\boldsymbol{u}_l \equiv \mathbf{0}$).

Finally, making use all of the bounds (32) to (35), it can be shown that

$$\|\bar{\boldsymbol{u}}_{ff} + \mathbf{W}\hat{\boldsymbol{\theta}}\| \leq \bar{W}_\theta \leq \underline{u} - \delta. \tag{36}$$

This concludes the proof. □

Corollary

If the desired relative trajectory $\boldsymbol{\rho}_d(t)$ is designed to satisfy (26) for some $\delta > 0$, then Assumption 4 is satisfied on the infinite interval $t \in [0, \infty)$ with the control law (17).

Proof

Suppose it were not the case, then by continuity of the solution, there must exist a time $t^* > 0$ and $0 < \delta_2 < \delta$, such that $\|\bar{\boldsymbol{u}}_{ff}(t^*) + \mathbf{W}\hat{\boldsymbol{\theta}}(t^*)\| = \underline{u} - \delta_2$, and $\|\bar{\boldsymbol{u}}_{ff}(t) + \mathbf{W}\hat{\boldsymbol{\theta}}(t)\| \leq \underline{u} - \delta_2$ on the interval $t \in [0, t^*]$, such that Assumption 4 is satisfied on this interval with δ_2. From the proof of Theorem 1, it is seen that $\boldsymbol{r}^T\boldsymbol{g}(\boldsymbol{r}, t) \leq 0$ on this interval. Therefore, from Lemma 2, it must be the case that $\|\bar{\boldsymbol{u}}_{ff}(t^*) + \mathbf{W}\hat{\boldsymbol{\theta}}(t^*)\| \leq \underline{u} - \delta < \underline{u} - \delta_2$ on this interval, which is a contradiction. Therefore, Assumption 4 must be satisfied on the infinite interval $t \in [0, \infty)$ with δ. □

Remark 3: The bound in (26) is a sufficient (and quite conservative) condition for Assumption 4 to hold. It can be used as a check for a given desired relative trajectory $\boldsymbol{\rho}_d(t)$, or as a design condition. It is not the purpose of this paper to demonstrate how to design $\boldsymbol{\rho}_d(t)$. However, there are a number of ways $\bar{W}_\theta$ in (27) can be reduced. By simply choosing $\boldsymbol{\rho}_d(0) = \boldsymbol{\rho}(0)$ and $\dot{\boldsymbol{\rho}}_d(0) = \dot{\boldsymbol{\rho}}(0)$, the bound $\bar{V}$ in (24) is minimized, and the terms containing $\boldsymbol{e}(0)$ in (27) are eliminated. Alternatively, the first term in (27) can be eliminated by choosing the desired trajectory $\boldsymbol{\rho}_d$ to be a natural motion under gravitational influences. This is desirable from the point of view of steady-state fuel consumption. There are several papers that address this last problem, [21, 22, 23] to name a few.

5 Numerical Example

As a numerical example to demonstrate the results in this paper, a two-spacecraft formation flying scenario is considered. The scenario is taken from [22]. Both spacecraft are under the influence of both two-body and J2 gravitational terms

[24]. The initial orbital elements of the leader spacecraft are

$$\begin{aligned} a &= 7078\ km \\ e &= 0 \\ i &= 60^o \\ \Omega &= 60^o \\ u &= 0^o \end{aligned}$$

The orbital period is approximately 5940s. In [22], initial conditions for the relative follower position were obtained that provide natural almost periodic motion. The resulting relative motion trajectory is the desired follower relative motion trajectory. From [22], the initial conditions of the desired trajectory are

$$\begin{aligned} \boldsymbol{\rho}_d(0) &= \begin{bmatrix} -375.22 & 5.499 & 27.712 \end{bmatrix}^T\ m \\ \dot{\boldsymbol{\rho}}_d(0) &= \begin{bmatrix} 0.011943 & 0.20637 & 0.41789 \end{bmatrix}^T\ m/s \end{aligned}$$

The leader spacecraft is uncontrolled, that is $\boldsymbol{u}_l = \mathbf{0}$. The disturbance forces acting on the leader and follower spacecraft are constant, and are given by $\boldsymbol{f}_l = \mathbf{0}$ and $\boldsymbol{f}_f = \begin{bmatrix} -1 \times 10^{-5} & 6 \times 10^{-5} & -2 \times 10^{-5} \end{bmatrix}^T\ N$ respectively. The mass of both spacecraft is $m_f = m_l = 50\ kg$. The controller parameters are

$$\begin{aligned} \mathbf{K} &= diag(50, 50, 50) \\ \boldsymbol{\Lambda} &= diag(10^{-3}, 10^{-3}, 10^{-3}) \\ \boldsymbol{\Gamma} &= diag(10^{-2}, 10^{-2}, 10^{-2}) \end{aligned}$$

The initial condition of the follower spacecraft is taken to coincide with the leader, that is $\boldsymbol{\rho}(0) = \mathbf{0}$ and $\dot{\boldsymbol{\rho}}(0) = \mathbf{0}$. The initial follower disturbance force estimate is $\hat{\boldsymbol{f}}_f = \mathbf{0}$. The known bound on the follower disturbance force is taken to be $\bar{\theta}_d = 10^{-4}$ N. To compute the bound in (25), only the dominant two-body

acceleration term was considered. With $\boldsymbol{a}_g(\boldsymbol{R}) = -\frac{\mu}{\|\boldsymbol{R}\|^3}\boldsymbol{R}$, it can be shown that

$$\left\| \frac{\partial \boldsymbol{a}}{\partial \boldsymbol{R}^T}(\boldsymbol{R}) \right\| \leq 4\frac{\mu}{\|\boldsymbol{R}\|^3}.$$

Since the desired relative trajectory is a natural trajectory under two-body and J2 gravitation, the first term in (27) is zero. Assuming that $\|\boldsymbol{R}_l\| \geq a - 100km$, the bound in (27) is now obtained as $W_\theta = 0.9709$ N. As mentioned in Remark 3, this bound is conservative, but guarantees that Assumption 4 is satisfied. It was found by trial and error that the saturation limits on the follower control effort could be reduced significantly without violating Assumption 4. Saturation limits were set at $u_{max} = 0.3$ N in each axis.

Three simulations were performed. The first is with the control law as described above including saturation constraints. The second is the same control law with the saturation constraints removed (this was shown in [10] to be asymptotically stable). The third is with no control.

Figures 2 to 8 show the simulation results. Figure 2 shows the follower position relative to the leader when the control law presented above is applied. Figures 3 to 5 shows the follower relative position error. It can be seen that the desired relative trajectory is obtained within one orbit when the control law is applied both with and without saturation constraints. Convergence is slightly lower when saturation constraints are in effect. Figures 3 to 5 also show that in the absence of control, the error does not converge, and displays a small secular drift due to the uncompensated disturbance force on the follower. Figures 6 and 7 show the initial time-history of the total follower control effort when saturation constraints are and are not enforced, respectively. It can be seen that in the absence of saturation constraints, the control law demands a very

large initial force, well outside the physical capability of the thrusters. When saturation constraints are enforced, the control law demands the full capacity of the thrusters for a more prolonged period of time, due to the slower convergence of the tracking error. Figure 6 suggests that the control input is non-zero at steady-state, as is required to overcome the disturbance force on the follower. Figure 8 shows the feedforward ($\bar{\boldsymbol{u}}_{ff} + \mathbf{W}\hat{\boldsymbol{\theta}}$) component of the follower control effort when saturation constraints are enforced. It is clear that Assumption 6 is never violated. In summary, as predicted by the theory, the desired formation is achieved in the presence of actuator saturation.

6 Conclusion

In this paper, the Slotine and Li adaptive controller has been applied to the multiple spacecraft formation flying problem, and examined in the context of actuator saturation. The formulation allows for gravitational field models of arbitrary order, and a broad class of linearly parameterized external disturbance force models. This controller is based upon the feedback of the filtered error. Making use of Barbalat's lemma, a broad class of controllers feeding back the filtered error has been obtained, which encompasses the linear feedback that is typically used. In particular, conditions have been presented under which the linear feedback is asymptotically stable under actuator saturation, such as would be present in a realistic scenario. The resulting controller performance has been demonstrated with a numerical example for a relative orbit under J2 perturbations.

References

[1] S. D'Amico, J.-S. Ardaens, S. De Florio, O. Montenbruck, Autonomous Formation Flying - TanDEM-X, PRISMA and Beyond, 5th International Workshop on Satellite Constellations & Formation Flying, Evpatoria, Crimea, 2-4 July, 2008.

[2] K. Yoshihara, M. van Mierlo, A. Ng, B. Shankar Kumar, A. de Ruiter, Y. Komatsu, H. Horiguchi, H. Hashimoto, JC2Sat-FF: An International Collaboration Nano-Sat Project - Overview of the System Analyses and Design, The 4S Symposium, Rhodes, Greece, 26-30 May, 2008.

[3] J. Eyer and C.J. Damaren, The stability analysis of a discrete-time control algorithm for the Canadian advanced nanospace eXperiment - 4 & 5 formation flying nanosatellites, *Proceedings of the Institution of Mechanical Engineers, Part G: Journal of Aerospace Engineering*, Vol. 223, No. 4, pp. 441-452, 2009.

[4] R.H. Vassar and R.B. Sherwood, Formationkeeping for a pair of satellites in a circular orbit, *Journal of Guidance, Control and Dynamics*, Vol. 8, No. 2, pp. 235–242, 1985.

[5] S.R. Vadali, S.S. Vaddi and K.T. Alfriend, An intelligent control concept for formation flying satellites, *International Journal of Robust and Nonlinear Control*, Vol. 12, No. 2-3, pp. 97–115, 2002.

[6] J.R. Carpenter, Decentralized control of satellite formations, *International Journal of Robust and Nonlinear Control*, Vol. 12, No. 2-3, pp. 141–161, 2002.

[7] W. Kang, A. Sparks and S. Banda, Coordinated control of multisatellite systems, *Journal of Guidance, Control and Dynamics*, Vol. 24, No. 2, pp. 360–368, 2001.

[8] P.K.C. Wang, F.Y. Hadaegh and K. Lau, Synchronized formation rotaiton and attitude control of multiple free-flying spacecraft, *Journal of Guidance, Control and Dynamics*, Vol. 22, No. 1, pp. 28–35, 1999.

[9] H.T. Liu, J. Shan and D. Sun, Adaptive Synchronization Control of Multiple Spacecraft Formation Flying, *ASME Journal of Dynamic Systems, Measurement and Control*, Vol. 129, No. 3, pp. 337–342, May 2007.

[10] M.S. de Queiroz, V. Kapila and Q. Yan, Adaptive Nonlinear Control of Spacecraft Formation Flying, *Journal of Guidance, Control and Dynamics*, Vol. 23, No. 3, pp. 385–390, May-June, 2000.

[11] J. Shan and H. Lin, Non-linear filter-based adaptive output feedback control for spacecraft formation flying, *Proceedings of the Institution of Mechanical Engineers, Part I: Journal of Systems and Control Engineering*, Vol. 223, No. 5, pp. 683–691, 2009.

[12] P. Gurfil, M. Ishan and N.J. Kasdin, Adaptive Neural Control of Deep-Space Formation Flying, *AIAA Journal of Guidance, Control and Dynamics*, Vol. 26, No. 3, pp. 491–501, May-June 2003.

[13] J.-J.E. Slotine and W. Li, Adaptive manipulator control: A case study, *IEEE Transactions on Automatic Control*, Vol. 33, No. 11, pp. 995–1003, 1988.

[14] J.-J.E. Slotine and M.D. Di Benedetto, Hamiltonian Adaptive Control of Spacecraft, *IEEE Transactions on Automatic Control*, Vol. 35, No. 7, pp. 848–852, 1990.

[15] T.I. Fossen, Comments on "Hamiltonian Adaptive Control of Spacecraft", *IEEE Transactions on Automatic Control*, Vol. 38, No. 4, pp. 671–672, 1993.

[16] R. Ortega and M.W. Spong, Adaptive Motion Control of Rigid Robots: a Tutorial, *Automatica*, Vol. 25, No. 6, pp. 877–888, 1989.

[17] D.M. Dawson, J. Hu and K. Lau, *Nonlinear Control of Electric Machinery*, Marcel Dekker, New York, 1998.

[18] P.C. Hughes, *Spacecraft Attitude Dynamics,* Dover Publications, New York, 2004.

[19] H. Schaub and J.L. Junkins, *Analytical Mechanics of Space Systems* AIAA Education Series, 2003.

[20] H.K. Khalil, *Nonlinear Systems,* 2nd Edition, Prentice Hall, Upper Saddle River NJ, 1996.

[21] H. Schaub and K.T. Alfriend, J_2 invariant relative orbits for spacecraft formations, *Celestial Mechanics and Dynamical Astronomy*, Vol. 79, No. 2,pp. 77-95, Feb. 2001

[22] C.J. Damaren, Almost periodic relative orbits under J2 perturbations, *Proceedings of the Institution of Mechanical Engineers, Part G: Journal of Aerospace Engineering*, Vol. 221, No. 5, pp. 767–774, 2007.

[23] P. Palmer and M. Halsall, Designing Natural Formations of Low-Earth-Orbiting Satellites, *Journal of Guidance, Control and Dynamics*, Vol. 32, No. 3, pp. 860–868, May-June 2009.

[24] D.A. Vallado, *Fundamentals of Astrodynamics and Applications,* 2nd Edition, Microcosm Press, El Segundo CA, 2004.

Appendix

Notation

$\boldsymbol{a}_g$	gravitational acceleration vector
$\boldsymbol{e}$	tracking error
$\boldsymbol{g}(\boldsymbol{r}, t)$	feedback law
$\boldsymbol{K}$	gain matrix
$\mathcal{L}_2$	space of all square integrable functions on $[0, \infty)$
m	spacecraft mass
$\boldsymbol{p}$	state vector
$\boldsymbol{r}$	filtered error
$\boldsymbol{R}$	absolute spacecraft inertial position
t	time
$\boldsymbol{u}$	control input
$\bar{\boldsymbol{u}}_{ff}$	feedforward control input
$\bar{\boldsymbol{u}}_f$	feedback control input
V	lyapunov-like function
$\mathbf{W}(\boldsymbol{\rho}, t)$	regressor matrix
δ	small positive number
$\boldsymbol{\Gamma}$	gain matrix
$\boldsymbol{\Lambda}$	gain matrix
$\boldsymbol{\omega}_o$	orbital angular velocity vector
$\boldsymbol{\rho}$	relative spacecraft position
$\boldsymbol{\theta}$	disturbance force parameterization vector
Subscripts	
f	follower
l	leader

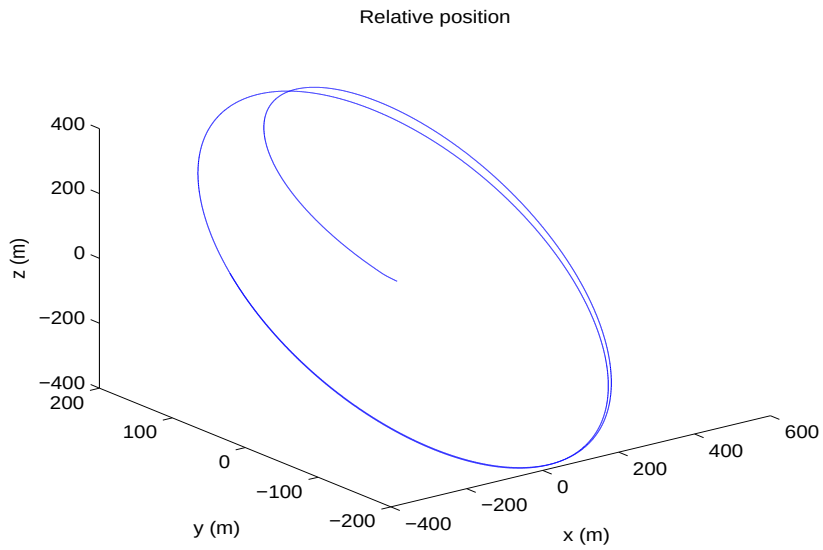

Figure 2: Follower Relative Orbit with Respect to Leader

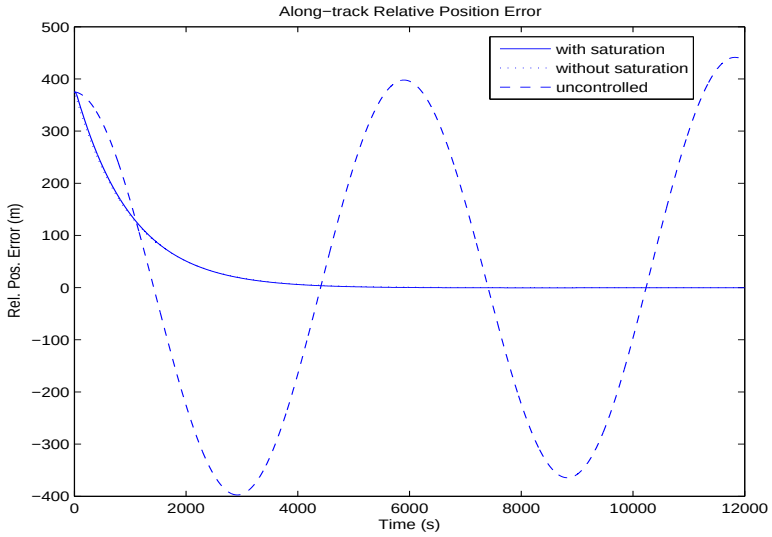

Figure 3: Along-track Follower Relative Position Error

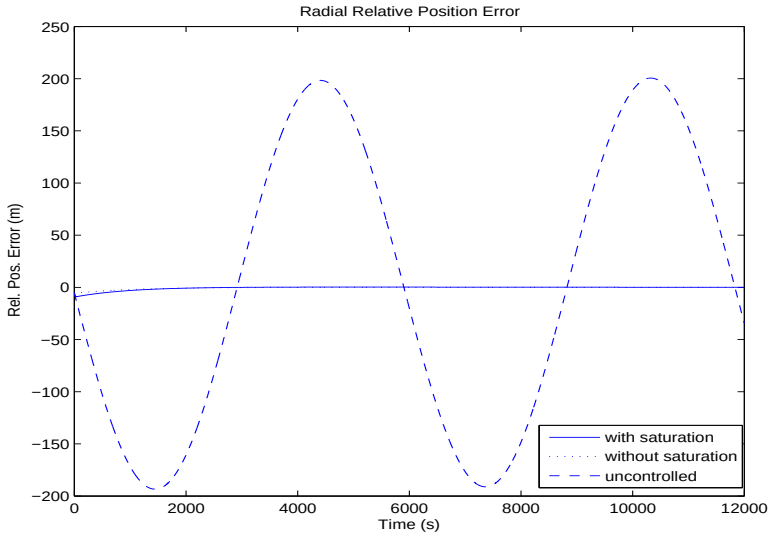

Figure 4: Radial Follower Relative Position Error

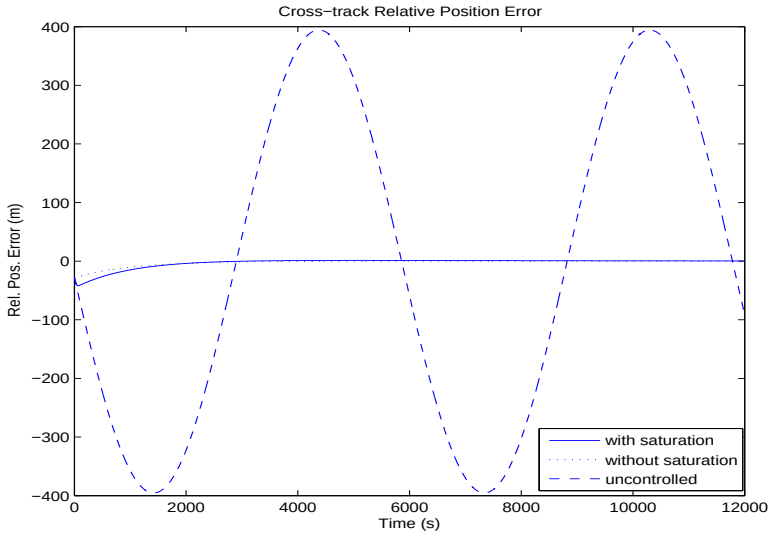

Figure 5: Cross-track Follower Relative Position Error

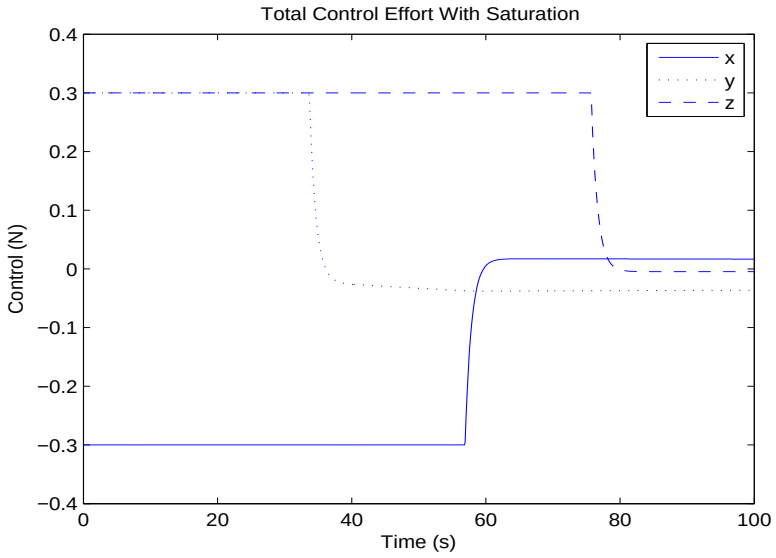

Figure 6: Total Follower Control Effort (With Saturation)

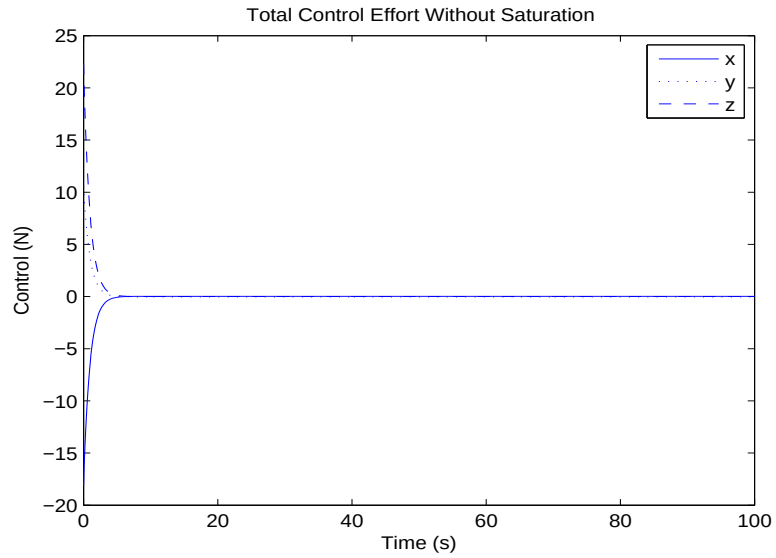

Figure 7: Total Follower Control Effort (Without Saturation)

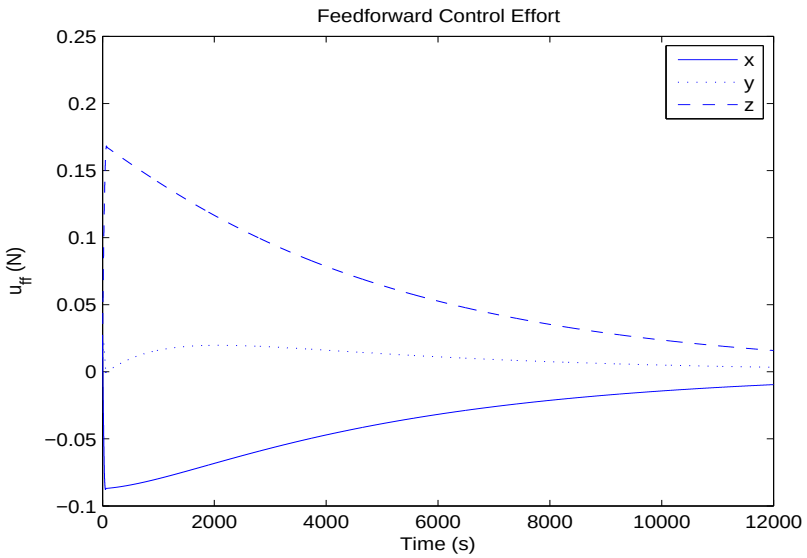

Figure 8: Follower Feedforward Control Effort ($\bar{\boldsymbol{u}}_{ff} + \mathbf{W}\hat{\boldsymbol{\theta}}$)